

This article was downloaded by:

On: 23 January 2011

Access details: *Access Details: Free Access*

Publisher *Taylor & Francis*

Informa Ltd Registered in England and Wales Registered Number: 1072954 Registered office: Mortimer House, 37-41 Mortimer Street, London W1T 3JH, UK



Journal of Coordination Chemistry

Publication details, including instructions for authors and subscription information:

<http://www.informaworld.com/smpp/title~content=t713455674>

Crystal structure and thermal decomposition kinetics of a 2D coordination polymer of cadmium(II)

Ying-Xia Zhou^a; Si-Yin Liu^b; Xiao-Qing Shen^c; Hong-Yun Zhang^c; Ya-Hui Yu^c

^a College of Science, Henan Agricultural University, Zhengzhou 450002, China ^b Department of Chemistry, Shangqiu Normal College, Shangqiu 476000, China ^c Department of Chemistry, Zhengzhou University, Zhengzhou 450052, China

To cite this Article Zhou, Ying-Xia , Liu, Si-Yin , Shen, Xiao-Qing , Zhang, Hong-Yun and Yu, Ya-Hui(2008) 'Crystal structure and thermal decomposition kinetics of a 2D coordination polymer of cadmium(II)', *Journal of Coordination Chemistry*, 61: 20, 3237 – 3244

To link to this Article: DOI: 10.1080/00958970802020665

URL: <http://dx.doi.org/10.1080/00958970802020665>

PLEASE SCROLL DOWN FOR ARTICLE

Full terms and conditions of use: <http://www.informaworld.com/terms-and-conditions-of-access.pdf>

This article may be used for research, teaching and private study purposes. Any substantial or systematic reproduction, re-distribution, re-selling, loan or sub-licensing, systematic supply or distribution in any form to anyone is expressly forbidden.

The publisher does not give any warranty express or implied or make any representation that the contents will be complete or accurate or up to date. The accuracy of any instructions, formulae and drug doses should be independently verified with primary sources. The publisher shall not be liable for any loss, actions, claims, proceedings, demand or costs or damages whatsoever or howsoever caused arising directly or indirectly in connection with or arising out of the use of this material.

Crystal structure and thermal decomposition kinetics of a 2D coordination polymer of cadmium(II)

YING-XIA ZHOU*†, SI-YIN LIU‡, XIAO-QING SHEN§,
HONG-YUN ZHANG§ and YA-HUI YU§

†College of Science, Henan Agricultural University, Zhengzhou 450002, China

‡Department of Chemistry, Shangqiu Normal College, Shangqiu 476000, China

§Department of Chemistry, Zhengzhou University, Zhengzhou 450052, China

(Received 15 June 2007; in final form 4 August 2007)

A 2D cadmium(II) coordination polymer with oxalate and 2,2'-bipyridine, $[\text{Cd}_2(\text{bpy})(\text{ox})_2(\text{H}_2\text{O})_2]_n \cdot n\text{H}_2\text{O}$, was synthesized and the single crystal structure was determined by X-ray crystallography. Thermal properties and the decomposition kinetics of the title complex were studied showing that the decomposition of this complex in N_2 is a two-step process, $A \xrightarrow{F_1} B \xrightarrow{F_2} C$. Kinetic parameters were obtained.

Keywords: Coordination polymer; Cadmium(II); Oxalate; Thermal decomposition kinetics

1. Introduction

The design and synthesis of metal coordination polymers have received considerable attention due to their architectures and potential applications in functional materials, nanotechnology, molecular recognition, etc. [1–3]. In the design and synthesis of metal coordination polymers, factors such as the structural characteristic of ligands, the metal ions and their coordination geometry, the inorganic counter anions, the ratio of metal-to-ligand and the reaction solvents [4–7] may influence the topological architectures and the properties of the coordination polymers obtained. The appropriate selection of metal centers and multifunctional ligands and the judicious choice of assembly reaction conditions may lead to formation of metal coordination polymers with new metal-ligand bonding modes and intriguing topological architectures.

In constructing metal coordination polymers, saturated aliphatic dicarboxylates such as malonate, oxalate, glutarate and malate [8–12] have been used as building blocks, owing to their conformational and coordination versatility. Among these, oxalate has been known to function as a bis-bidentate ligand, binding metal ions in diverse bonding modes leading to formation of polynuclear complexes ranging from discrete entities to multidimensional systems [13–17]. Large numbers of coordination polymers containing

*Corresponding author. Email: sherrly1992@sina.com

oxalate with interesting compositions and topologies have been synthesized through introducing N-donor ligands such as 2,2'-bipyridine, 4,4'-bipyridine and phenanthroline [18–21] into the reaction systems.

In this contribution, a 2D mixed-ligand cadmium(II) polymer with oxalate and 2,2'-bipyridine co-ligands, $[\text{Cd}_2(\text{bpy})(\text{ox})_2(\text{H}_2\text{O})_2]_n \cdot n\text{H}_2\text{O}$ (bpy = 2,2'-bipyridine, $\text{ox} = \text{C}_2\text{O}_4^{2-}$), was synthesized. The single crystal structure was determined by X-ray crystallography, the thermal properties investigated by thermogravimetry (TG) and the decomposition kinetics studied by an un-isothermal method.

2. Experimental

2.1. Synthesis of title complex

One mmol 2,2'-bipyridine in EtOH aqueous (20 mL, 1:1) was added to 1.5 mmol $\text{Cd}(\text{NO}_3)_2 \cdot 4\text{H}_2\text{O}$ aqueous solution (5 mL) under stirring for 1 h. Then 1.5 mmol oxalic acid aqueous solution (10 mL) was added to the mixture. After being refluxed for 1 h, the resulting solution was allowed to stand at ambient temperature. After several weeks, colorless crystals were obtained, collected by filtration, washed with water and dried under vacuum. Yield: 53%. Found: C, 27.59; H, 2.31; N, 4.60%. Calcd for $\text{C}_{14}\text{H}_{14}\text{Cd}_2\text{N}_2\text{O}_{11}$: C, 27.49; H, 2.29; N, 4.58%. IR(KBr cm^{-1}): 3412m, 3072w, 1647s, 1583w, 1515w, 1424m, 866w, 727m.

2.2. Physical measurements

Elemental analyses were performed on a Perkin-Elmer 240C analyzer and IR spectra were recorded on a Nicolet IR-470 spectrometer using KBr pellets in the range 4000–400 cm^{-1} . Thermal decomposition experiments were carried out using a Netzsch TG 209 instrument in nitrogen atmosphere. The heating rate for thermal decomposition was 10°C min^{-1} .

Data collection was made using graphite monochromated Mo-K α ($\lambda = 0.071073$ nm) radiation on a Rigaku Raxis-IV X-ray diffractometer at 291(2) K. The structures were solved by direct methods and refined on F^2 by full-matrix least squares using SHELXTL [22]. Non-hydrogen atoms were located by direct phase determination and subjected to anisotropic refinement. All the hydrogen atoms were placed in calculated positions. Details of the crystal structure determination of the title complex are listed in table 1, and selected bond distances and angles in table 2.

3. Results and discussion

3.1. Structure of title complex

The structure of the title complex is shown in figure 1. Cd1 is six-coordinate by four oxygen atoms from two $\text{C}_2\text{O}_4^{2-}$ ions and two nitrogen atoms of 2,2'-bipyridine, forming a distorted octahedral geometry; Cd2 is 7-coordinate with four oxygen atoms from two

Table 1. Crystallographic data and refinement parameters for the title complex.

Formula	C ₁₄ H ₁₄ Cd ₂ N ₂ O ₁₁
Formula weight	611.07
Crystal system	Monoclinic
Space group	<i>P</i> 2(1) <i>n</i>
Unit cell dimensions (Å, °)	
<i>a</i>	7.7884(16)
<i>b</i>	15.030(3)
<i>c</i>	15.661(3)
α	90
β	93.89(3)
γ	90
Volume (Å ³)	1829.0(6)
<i>Z</i>	4
<i>D</i> _{Calcd} (Mg m ⁻³)	2.219
<i>F</i> (000)	1184
Reflections collected/unique	5521/3030 [<i>R</i> (int) = 0.0186]
Goodness-of-fit on <i>F</i> ²	1.051
Final <i>R</i> indices [<i>I</i> > 2σ(<i>I</i>)]	<i>R</i> ₁ = 0.0304; <i>wR</i> ₂ = 0.0837

Table 2. Selected bond distances (Å) and angles (°) for the title complex.

Cd(1)–O(5)	2.280(3)	Cd(2)–O(9)	2.244(4)
Cd(1)–O(2)	2.295(3)	Cd(2)–O(10)	2.343(4)
Cd(1)–O(1)	2.304(3)	Cd(2)–O(3)	2.353(3)
Cd(1)–O(6)	2.304(3)	Cd(2)–O(8)#1	2.371(3)
Cd(1)–N(2)	2.318(4)	Cd(2)–O(7)#1	2.420(3)
Cd(1)–N(1)	2.385(4)	Cd(2)–O(4)	2.421(3)
O(4)–Cd(2)#2	2.539(3)	Cd(2)–O(4)#2	2.539(3)
O(7)–Cd(2)#3	2.420(3)	O(8)–Cd(2)#3	2.371(3)
O(5)–Cd(1)–O(2)	87.65(12)	O(5)–Cd(1)–O(6)	72.39(12)
O(5)–Cd(1)–O(1)	111.26(13)	O(2)–Cd(1)–O(6)	139.88(14)
O(2)–Cd(1)–O(1)	71.36(11)	O(1)–Cd(1)–O(6)	83.74(12)
O(2)–Cd(1)–N(2)	97.62(14)	O(5)–Cd(1)–N(2)	156.16(14)
O(9)–Cd(2)–O(3)	141.17(12)	O(3)–Cd(2)–O(8)#1	103.74(13)
O(10)–Cd(2)–O(3)	85.43(14)	O(9)–Cd(2)–O(7)#1	80.16(14)
O(9)–Cd(2)–O(8)#1	94.13(14)	O(10)–Cd(2)–O(7)#1	140.34(12)
O(10)–Cd(2)–O(8)#1	150.24(13)	O(3)–Cd(2)–O(7)#1	74.74(12)
O(3)–Cd(2)–O(4)#2	138.81(11)	O(8)#1–Cd(2)–O(7)#1	69.08(11)

Symmetry transformations used to generate equivalent atoms: #1. $-x+1/2, y-1/2, -z+1/2$; #2. $-x+1, -y+2, -z$; #3. $-x+1/2, y+1/2, -z+1/2$.

C₂O₄²⁻ ions and two water molecules together with a bridging O atom (O4) from another oxalate ion. As for the oxalate ligand, there are two coordination modes, one is chelate *bis*-bidentate, another is chelate bidentate and chelate/bridging bidentate, a new mode as far as we know. Furthermore, Cd2 and Cd2A assemble in opposite direction, which results in a centrosymmetric structure unit [Cd₄(bpy)₂(ox)₄(H₂O)₄] (see figure 1). Two Cd2 atoms (Cd2, Cd2A) are connected to each other through two bridging O atoms (O4, O4A) from two oxalate ligands to form a parallelogram. A similar connecting fashion can be seen in [Cd₂L₂(H₂O)₂Br₄]_n·2nH₂O (L = 2,2'-*bis*(4-pyridylmethyleneoxy)-1,1'-*bi*-naphthalene) with bridging Br⁻ [19], but Cd in that polymer has only one coordination mode.

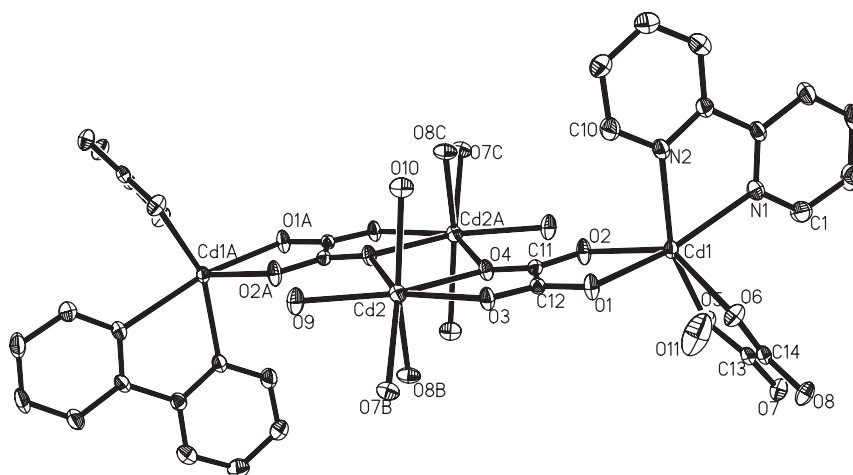


Figure 1. ORTEP drawing of the title complex (with 50% probability displacement ellipsoids).

A pronounced conformational feature of the structure is that 16 atoms (Cd2, Cd2A, O4, O4A, O1, O1A, O2, O2A, C11, C11A, O3, O3A, O9, O9A) are coplanar with mean deviation of 0.0529 Å, and Cd1 atoms (Cd1, Cd1A) are slightly out of the plane due to chelation of $C_2O_4^{2-}$ ions and 2,2'-bipyridine. The 2,2'-bipyridine plane is almost vertical to this big plane with a dihedral angle of 91.7°, and this arrangement leads to formation of a framework constructed by $C_2O_4^{2-}$ and Cd (see figure 2a) with 2,2'-bipyridine in it. This configuration together with the radius of coordinated oxalate make the 2D layer look like superposed, interlaced and closed curves connected with 2,2'-bipyridine (figure 2b). In addition, hydrogen bonds exist between oxalate O atoms and water molecules, including coordinated H_2O and lattice H_2O ; those in adjacent layers give rise to a 3D supramolecular H-bonding framework.

3.2. Thermal stabilities and thermal decomposition kinetics

The typical DSC and TG curves of the title complex are shown in figures 3 and 4, respectively. Three transitions appeared in the decomposition process. The first transition from 95.0 to 200°C with DSC peak at 183°C is due to the loss of lattice and coordinated H_2O from the structure. The higher temperature value and wide temperature range for water loss is caused by the participation of coordinated water in complicated hydrogen bonds. The calculated mass loss of 9.07% for this thermal event agrees with that revealed by the TG curve (8.84%).

The second transition from 200 to 400°C is a consecutive complicated process containing two contiguous DTG peaks at 325 and 355°C. This thermal event is an endothermic process with ΔH of 356.2 Jg⁻¹ in the DSC curve, due to decomposition of $C_2O_4^{2-}$ and 2,2'-bipyridine, and accompanied by formation of CdO. The third transition is beyond 400 and is related to the gradual elimination of carbon from $[Cd_2(bpy)(ox)_2]_n$ decomposition in N_2 [23]. The total mass loss of 78.28% up to 680°C is quite closed to the theoretical value (78.98%) calculated by taking CdO as the final product. The second transition is more important and will be taken in to kinetic analysis.

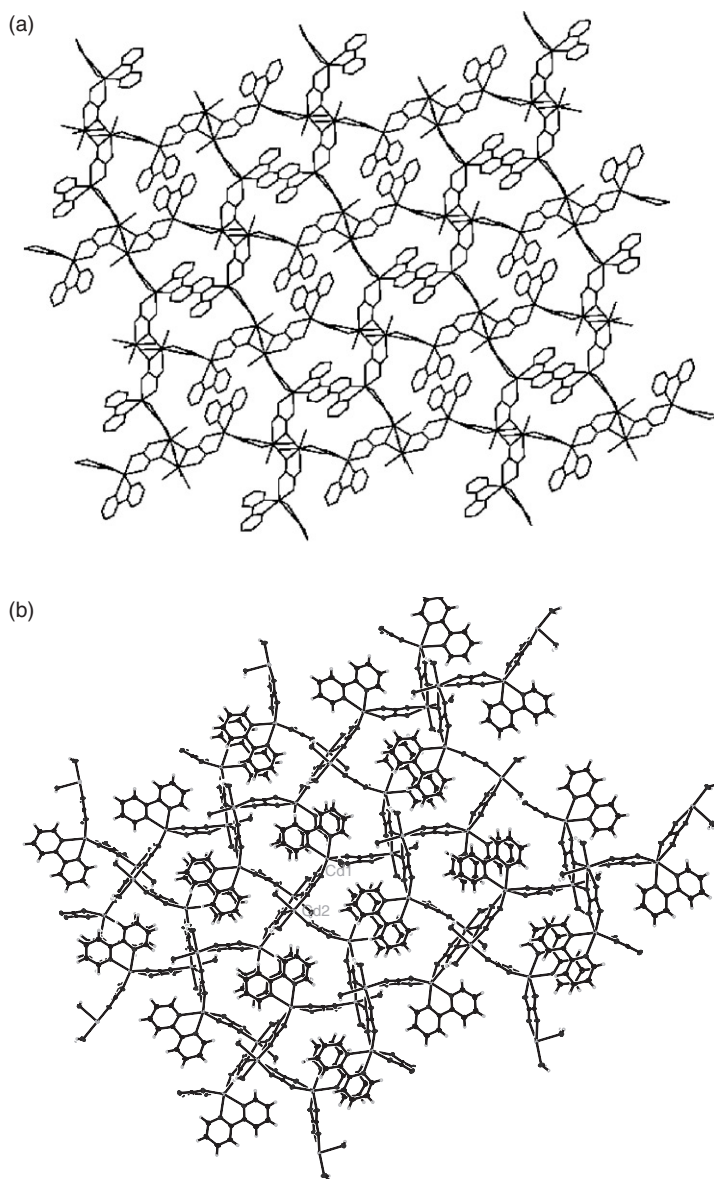


Figure 2. (a) 2D infinite framework of the complex. The O atoms of lattice H₂O are omitted for clarity; (b) 2D infinite framework of superposed, interlaced curves viewed along the *a*-axis. The lattice H₂O is omitted for clarity.

According to the non-isothermal kinetics theory of Ozawa–Flynn–Wall (OFW), kinetic parameters can be obtained from the equation below [24],

$$\ln \beta = \ln \left(\frac{AE}{R} \right) - \ln g(\alpha) - 5.3305 - 1.052 \cdot \frac{E}{RT} \quad (1)$$

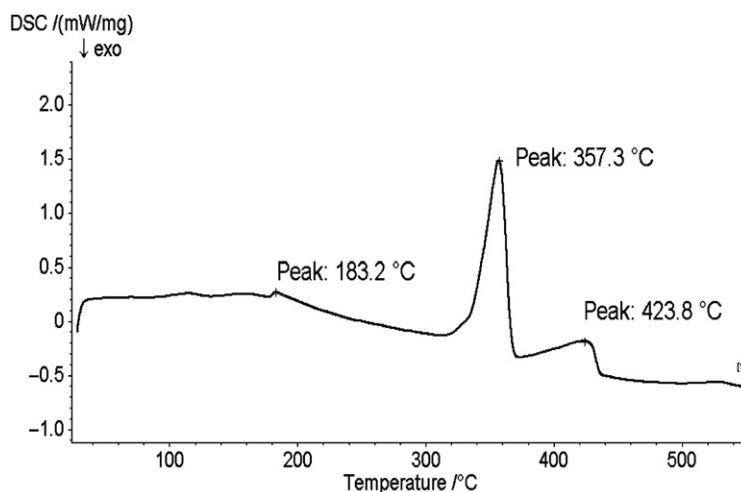


Figure 3. DSC curve of the title complex.

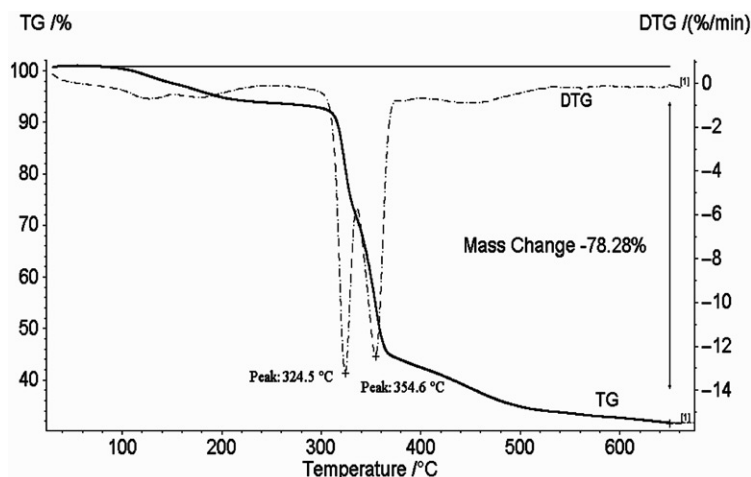


Figure 4. TG-DTG curve of the title complex.

where β is heating rate, α degree of conversion, $g(\alpha)$ mechanism function, E activation energy, A pre-exponential factor, and R gas constant.

With different heating rates of 5, 10, 20 and 30 °C min⁻¹, different temperature data are obtained in the same degree of conversion (α). These data are used in equation (1), from which it is seen that graphs of $\ln \beta$ versus $1/T$ show straight lines with slopes $m = -1.052E/R$. Figure 5 shows the activation energy (E) with different α . The appearance of two maxima indicates decomposition is a double step reaction. Selecting mechanism function $f(\alpha)$ of different singular reaction types [25], testing all two-step reaction types, and setting the initial values of the parameters of E according to figure 5, the calculated curves were obtained by means of multivariate non-linear regression. These curves were fitted to the experimental ones and corrected with least squares method. Considering fitting quality, the mechanism of $d:f, A \xrightarrow{Fn} B \xrightarrow{Fl} C$,

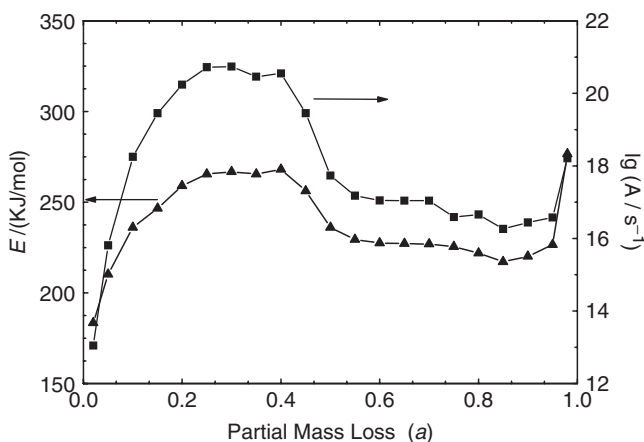
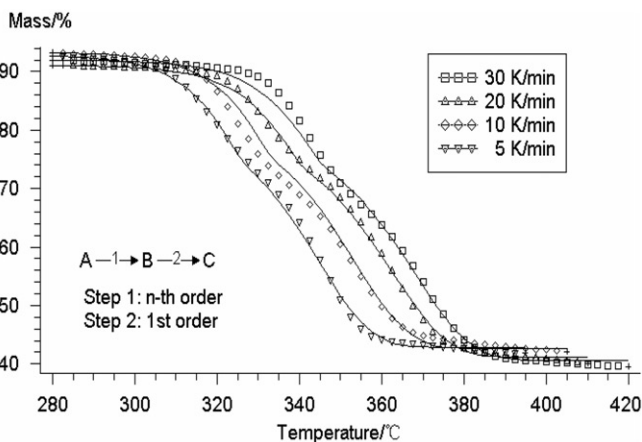
Figure 5. Activation energy (E) and $\lg A$ at different α .

Table 3. Kinetic data and fitting quality on the complex.

Corr. Coeff.	Reg. Par.	Step	Mode	$E(\text{kJ mol}^{-1})$	$\lg(A/\text{s}^{-1})$	Order
0.998839	0.00100	I	$F1$	138.7386	12.3349	
		II	F_n	291.0868	23.2351	2.2982

Figure 6. Curve fitting of second transition, simulated with reaction types F_n and $F1$. ∇ , \diamond , Δ , \square experimental plots, — integral plots.

is the most suitable for this reaction. The optimized kinetic parameters are obtained (see table 3) and graphic presentation of the curve fitting is shown in figure 6. From figure 6 it can be seen that the experimental data and the nonlinear regression model fit very well with correlation coefficient above 0.999.

In short, the kinetic analysis above shows that the decomposition of the title complex is a two-step reaction $A \xrightarrow{F_n} B \xrightarrow{F1} C$: an n -th order reaction (F_n) with $n=0.36$,

$E1 = 278.2 \text{ kJ mol}^{-1}$, $\log(A1/s^{-1}) = 22.3$, is followed by a 1st order reaction ($F1$) with $E2 = 244.6 \text{ kJ mol}^{-1}$, $\log(A2/s^{-1}) = 18.5$.

Supplementary material

The supplementary crystallographic data for this article can be obtained free of charge from The Director, CCDC, 12 Union Road, Cambridge CB2 1EZ, UK (Fax: +44-1223-336-033; Email: deposit@ccdc.cam.ac.uk or www: http://www.ccdc.cam.ac.uk). CCDC Reference No.: 272864.

Acknowledgement

This work was financially supported by the National Science Foundation of China (20501017).

References

- [1] O. Oms, J.L. Bideau, F. Leroux, A. Lee, D. leclercq, A. Vioux. *J. Am. Chem. Soc.*, **126**, 12090 (2004).
- [2] N. Singh, R.K. Sinha. *Inorg. Chem. Commun.*, **5**, 255 (2002).
- [3] H. Li, M. Eddaoudi, M. O'Keeffe, O.M. Yaghi. *Nature.*, **402**, 276 (1999).
- [4] Y.Q. Gong, R.H. Wang, Y.F. Zhou, D.Q. Yuan, M.C. Hong. *J. Mol. Struct.*, **705**, 29 (2004).
- [5] A.J. Blake, N.R. Champness, P. Hubberstey, W.S. Li, M. Schröder, M.A. Withersby. *Coord. Chem. Rev.*, **183**, 117 (1999).
- [6] M.A. Withersby, A.J. Blake, N.R. Champness, P.A. Cooke, P. Hubberstey, W.S. Li, M. Schröder. *Inorg. Chem.*, **38**, 2259 (1999).
- [7] P.J. Hagrman, D. Hagrman, J. Zubietta. *Angew. Chem. Int. Ed.*, **38**, 2638 (1999).
- [8] L.S. Long, X.M. Chen, M.L. Tong, Z.G. Sun, Y.P. Ren, R.B. Huang, L.S. Zheng. *J. Chem. Soc., Dalton Trans.*, 2888 (2001).
- [9] E.W. Lee, Y.J. Kim, D.Y. Jung. *Inorg. Chem.*, **41**, 501 (2002).
- [10] R. Vaidhyanathan, S. Natarajan, C.N.R. Rao. *J. Chem. Soc., Dalton Trans.*, 1459 (2003).
- [11] C. Livage, C. Egger, G. Férey. *Chem. Mater.*, **11**, 1546 (1999).
- [12] Y. Guo, D. Xiao, E. Wang, Y. Lu, J. Lü, X. Xu, L. Xu. *J. Solid State Chem.*, **178**, 776 (2005).
- [13] J.C. Dai, X.T. Wu, Z.Y. Fu, C.P. Cui, S.M. Hu, W.X. Du, L.M. Wu, H.H. Zhang, R.Q. Sun. *Inorg. Chem.*, **41**, 1391 (2002).
- [14] H. Grove, J. Sletten, M. Julve, F. Lloret, L. Lezama, J. Carranza, S. Parsons, P. Rillema. *J. Mol. Struct.*, **606**, 253 (2002).
- [15] O. Castillo, A. Luque, F. Lloret, P. Roman. *Inorg. Chem. Commun.*, **4**, 350 (2001).
- [16] B. Kamenar, B. Kaitner, N. Strukan. *Croat. Chem. Acta*, **64**, 329 (1991).
- [17] Y.C. Jiang, S.L. Wang, S.F. Lee, K.H. Lii. *Inorg. Chem.*, **42**, 6154 (2000).
- [18] A.C. Fabretti, G. Franchini, P. Zannini, M.D. Vaira. *Inorg. Chim. Acta*, **105**, 187 (1985).
- [19] Y.Q. Gong, Y.F. Zhou, L. Han. *J. Mol. Struct.*, **748**, 195 (2005).
- [20] J. Tang, E. Gao, W. Bu, D. Liao, S. Yan, Z. Jiang, G. Wang. *J. Mol. Struct.*, **252**, 271 (2000).
- [21] S.Q. Xia, S.M. Hu, J.C. Dai, X.T. Wu, Z.Y. Fu, J.J. Zhang, W.X. Du. *Polyhedron*, **23**, 1003 (2004).
- [22] G.M. Sheldrick. *Acta Crystallogr., Sect. A*, **46**, 467 (1990).
- [23] X.Q. Shen, H.J. Zhong, H.Y. Zhang, H.Y. Mao, Q.A. Wu, Y. Zhu. *Polyhedron*, **23**, 876 (2004).
- [24] T. Ozawa. *Bull. Chem. Soc. Japan*, **38**, 1881 (1965).
- [25] C.H. Bamford, C.F. Tipper (Eds). *Comprehensive Chemical Kinetics*, Vol. 22, P. 57, Reactions in Solid State, Elsevier, Amsterdam (1980).